

---

# ATOMWORLD: A BENCHMARK FOR EVALUATING SPATIAL REASONING IN LARGE LANGUAGE MODELS ON CRYSTALLINE MATERIALS

**Taoyuze Lv**

Suzhou Institute for Advanced Research  
University of Science and Technology of China  
taoyuze.lv@ustc.edu.cn

**Alexander Chen**

University of New South Wales  
alex.chen@student.unsw.edu.au

**Fengyu Xie\***

Suzhou Institute for Advanced Research  
University of Science and Technology of China  
fengyu\_xie@ustc.edu.cn

**Chu Wu**

Suzhou Institute for Advanced Research  
University of Science and Technology of China  
ljc001122@mail.ustc.edu.cn

**Jeffrey Meng**

University of New South Wales  
jeffrey.meng@unsw.edu.au

**Dongzhan Zhou**

Shanghai Artificial Intelligence Laboratory  
zhoudongzhan@pjlab.org.cn

**Yingheng Wang**

Cornell University  
yingheng@cs.cornell.edu

**Bram Hoex**

University of New South Wales  
b.hoex@unsw.edu.au

**Zhicheng Zhong**

Suzhou Institute for Advanced Research  
University of Science and Technology of China  
zczhong@ustc.edu.cn

**Tong Xie\***

University of New South Wales  
Green Dynamics  
tong.xie@unsw.edu.au

## ABSTRACT

Large Language Models (LLMs) excel at textual reasoning and are beginning to develop spatial understanding, prompting the question of whether these abilities can be combined for complex, domain-specific tasks. This question is essential in fields like materials science, where deep understanding of 3D atomic structures is fundamental. While initial studies have successfully applied LLMs to tasks involving pure crystal generation or coordinate understandings, a standardized benchmark to systematically evaluate their core reasoning abilities across diverse atomic structures has been notably absent. To address this gap, we introduce the AtomWorld benchmark to evaluate LLMs on tasks based in Crystallographic Information Files (CIFs), a standard structure representation format. These tasks, including structural editing, CIF perception, and property-guided modeling, reveal a critical limitation: current models, despite establishing promising baselines, consistently fail in structural understanding and spatial reasoning. Our experiments show that these models make frequent errors on structure modification tasks, and even in the basic CIF format understandings, potentially leading to cumulative errors in subsequent analysis and materials insights. By defining these standardized tasks, AtomWorld lays the ground for advancing LLMs toward robust atomic-scale modeling, crucial for accelerating materials research and automating scientific workflows.

<https://github.com/theAfish/AtomWorldBench>

---

\*Corresponding author

---

## 1 INTRODUCTION

A Crystallographic Information File (CIF) (Hall et al., 1991) is the standard format for storing crystallographic structural data. At the most basic level, a CIF can model the ideal, periodic arrangement of atoms in a bulk material. For more realistic scenarios, CIFs can also model defects, molecules in defect sites, stacked heterostructures, etc. Suppose that there are three stages for an LLM to reason with CIF files: **motor skills**, **perceptual skills** and **cognitive skills**. **Motor skills** are about the mechanics of geometry - being able to add, move, rotate, or insert atoms consistently within a structure. **Perceptual skills** are about recognising patterns - seeing motifs, detecting symmetry or connectivity, and being able to relate this structure to material properties. **Cognitive skills** are about reasoning and creativity - engaging in hypothesis-driven modifications and proposing novel structures.

LLMs for material discovery would primarily benefit researchers at the cognitive stage. Several works such as CrystaLLM, MatterGPT, and AtomGPT (Antunes et al., 2024; Chen et al., 2024; Choudhary, 2024) aim to leverage the generative capability of LLMs to generate useful and novel CIFs. These works however, are fundamentally limited by the scope of pretraining data - generations are plausible mostly only for data-rich domains of ideal, bulk crystals. The hypothesis which motivates our work is that LLMs could generate useful CIFs past data-rich domains if the more tractable problem of CIF modification is solved as opposed to ab initio generation. Learning CIF modification is learning *how* rather than *what* to generate, requiring both motor and perceptual skills as a prerequisite. In current literature, perceptual skills have been tested through question-answer (QA) style benchmarks e.g. LLM4Mat-Bench (Niyongabo Rubungo et al., 2025), but less attention has been given to testing motor skills. To address this gap, our research question asks: how can we measure and improve LLM “crystallographic motor skills”, i.e. ability to manipulate atoms in crystal structures?

In this work we introduce **AtomMotor-1K**, a compact test set of 1500 questions to benchmark reasoning LLMs on CIF motor skills. The test is made of 10 CIF action types, broken down from the real-world structural modifications which researchers may perform on CIFs. To the best of our knowledge, this is the first benchmark which examines this fundamental skill of crystallography in LLMs. The dataset of AtomMotor-1K was generated from our **AtomWorld data generator**, which can generate unlimited samples for each action, and also be used to support LLM training. We used AtomMotor-1K to evaluate several frontier text-based models, which through algorithmic approaches were generally able to succeed at simpler tasks such as adding or moving atoms, but struggled with more complex tasks such as rotating around an atom. Notably, some actions intuitive to humans had high error rates, while others considered more tedious were solved unexpectedly well. Furthermore, for the analysis of AtomMotor-1K we designed a series of tests (PointWorld, CIF-Gen, CIF-Repair, Chemical Competence Score, Struct-Prop) to isolate different aspects of LLM weaknesses and explore the relation that motor skills tests have with perceptual and cognitive skills.

We expect AtomWorld and AtomMotor-1K to gain increasing relevance as LLMs improve. LLMs have traditionally struggled with the spacial reasoning and long syntax following skills required by our benchmark - but this may soon change with rapid advancements in tool-augmented design (Hu et al., 2025), diffusion LLMs (Nie et al., 2025; Song et al., 2025), and as language-aligned video generation (Zheng et al., 2024; DeepMind, 2025) and robotics (Assran et al., 2025) models become increasingly capable. LLMs capability to manipulate crystal geometries is an important yet underexplored topic, and we believe the AtomWorld playground can play a foundational role in both testing and developing this in tomorrow’s LLMs.

## 2 RELATED WORK

**LLMs for crystallography.** LLMs have been primarily explored for their capabilities in CIF generation and QA. LLMs have been demonstrated to hold an innate ability to generate crystal structures when pretrained on millions of CIF files (Antunes et al., 2024). This process may be further reinforced through evolutionary search frameworks (Gan et al., 2025). However, as LLMs are pattern predictors, the search space is fundamentally limited by the scope of the pretraining data. LLMs can also be instruction fine-tuned to predict crystal properties or provide general QA responses from CIF, e.g. AlchemBERT, NatureLM, Darwin 1.5, etc (Liu et al., 2025; Xia et al., 2025; Xie et al., 2025; Van Herck et al., 2025; Nate Gruver & Ulissi, 2024). In data modelling, MatText (Alampara

---

et al., 2025) investigates if such QA can be improved through different textual representations. Crystallography QA is well benchmarked, with the most comprehensive being LLM4Mat-Bench (Niyongabo Rubungo et al., 2025), consisting of approximately 2 million composition-structure-description pairs. Crystallography benchmarks also cover multimodal LLMs, e.g. work by Polat et al. (2025) investigates the generation of structural annotations to crystallographic images.

Tool-augmented LLMs such as OSDA Agent (Hu et al., 2025) improve structure generation through coupling computational chemistry tools to LLMs. These tool-augmented design frameworks are able to address the lack of in-depth chemistry knowledge of LLMs without expensive (and not always effective) fine-tuning. LLMs may be able to reliably handle geometric CIF modification through tool-augmentation.

**Multimodal reasoning.** Approaches such as multimodal chain-of-thought (Multimodal-CoT) and visualization-of-thought (VoT) (Zhang et al., 2024; Wu et al., 2024) add image modalities to the reasoning trace rather than pure textual chain-of-thought. In particular, Multimodal-CoT with under 1 billion parameters achieved state of the art in state-of-the-art performance on the ScienceQA benchmark, outperforming larger models like GPT-3.5. As CIF describes a 3D challenge, these results suggest that multimodal reasoning approaches can be highly applicable to improving LLM ability on CIF geometry tasks, as well as reasoning-intensive QA and structure generation/modification tasks. Approaches to multimodal representation may also be influenced from developments in video generation and robotics, where models such as Genie 3 and V-JEPA 2 (DeepMind, 2025; Assran et al., 2025) are increasingly capable of understanding real-world physics and integrating this with natural language input/output. Finally, with the training objective of diffusion LLMs (Nie et al., 2025; Song et al., 2025) to be noise reversal, they have an advantage in understanding structural text compared to autoregressive LLMs - with LLaDA (Nie et al., 2025) surpassing GPT-4o in a reversal poem completion task. This also suggests diffusion LLMs may be inherently capable of differentiating between valid and invalid modifications to CIF - important for geometric modification tasks. Developments in multimodal reasoning and diffusion suggest that LLMs may be on the cusp of being able to grasp the 3D CIF environment, making it important to benchmark this progress.

### 3 PLAYGROUND DESIGN: ATOMWORLD

#### 3.1 ATOMWORLD GENERATOR

The dataset of AtomMotor-1K was generated from the scalable AtomWorld data generator. The data follows a three-part structure: two CIF files of “before” and “after” states, and an action prompt describing the change - with the goal of the LLM to yield the “after” state, given the “before” state and action. A flowchart describing the workflow from data generator to benchmark is presented in Figure 1.

The CIF format contains many optional and extensible fields. Using arbitrarily mixed CIF variants would introduce additional sources of uncertainty that are not directly related to the manipulation abilities we intend to evaluate. For this reason, we adopt the default CIF representations generated from *pymatgen* (Ong et al., 2013) and the Materials Project (MP) (Jain et al., 2013) as a standardized input format for all tasks. We leave studying how LLM performance varies across different CIF styles, as well as across other structure formats such as POSCAR and XYZ for future work.

All actions currently supported by AtomWorld are detailed in Table 1. These actions are designed to be translatable into the real-world structural modifications which researchers may perform, e.g.:

- Point defect & Doping: `change`, `remove`, `add`, `insert_between`, `swap`
- Surface generation: `delete_below`
- Structure perturbation: `move`, `move_towards`, `rotate_around`
- Supercell creation: `super_cell`

#### 3.2 ATOMWORLD FOR LLM TRAINING

The AtomWorld playground can be used to generate data suitable for LLM training, for instance the three-part structure of CIF-before + Action Prompt to CIF-after could feed directly into LLM

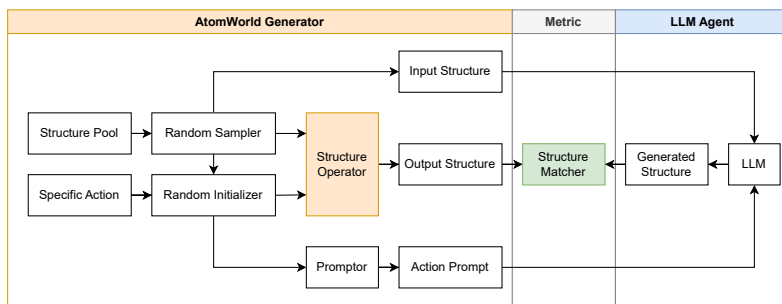


Figure 1: AtomWorld benchmark flowchart. The AtomWorld generator follows a structured data flow: the random sampler selects a structure from a predefined structure pool; the random initializer parametrizes the chosen action template by assigning atom indices and/or positions; the structure operator applies the instantiated action to the original structure to obtain the target structure; and the prompter generates a natural language description aligned with the action. The resulting (input structure, action prompt) pairs are then fed into the LLM agent system, whose generated structure is compared against the target structure using the `StructureMatcher` from *pymatgen* to compute the desired evaluation metric.

Table 1: Actions and the corresponding Action Prompt for AtomWorld.

Action name	Action prompt
change	Change the atom at index {index} into {new_symbol} in the cif file. The indices of atoms are started from 0.
remove	Remove the atom at index {index} from the cif file. The indices of atoms are started from 0.
add	Add one {symbol} atom at the Cartesian coordinate {position} to the cif file.
move	Move the atom at index {index} by {d_pos} angstrom in the cif file.
move_towards	Move the atom at index {index1} towards the atom at index {index2} by {distance} angstrom in the cif file.
insert_between	Insert a {symbol} atom in the line between atoms at indices {index1} and {index2}, and the inserted atom must be {distance:.2f} angstrom from atom at {index1} in the cif file.
swap	Swap the spatial positions of atoms at indices {index1} and {index2} in the cif file. The indices of atoms are started from 0.
delete_below	Delete all atoms whose z coordinate is lower than the atom at index {index} in the cif file. Excluding itself and atoms with the same z coordinate.
rotate_around	Rotate all surrounding atoms within {radius} angstrom of the center atom at index {index} by {angle} degree around the axis {axis} in the cif file. The rotation should following the right-hand rule.
super_cell	Create a supercell with the size {dim_0}x{dim_1}x{dim_2}.

pretraining. Alternatively, the same evaluation metric for AtomWorld benchmark could be used as the learning reward for reinforcement learning (RL). We leave LLM training for future work.

### 3.3 COMPLEMENTARY TESTS

To support the analysis of AtomMotor-1K, we design a set of complementary tests spanning format literacy, spatial reasoning, and property-oriented understanding. These tests play the role of breaking down AtomMotor-1K to systematically target different levels of reasoning, and also to tease the applicability of agentic CIF modification workflows through integrating tests for perceptual skills.

1. **PointWorld:** A stripped-down variant of AtomWorld for measuring the inherent difficulty of each geometric operation. Structures are represented as a set of points in three-dimensional

---

space, expressed in raw coordinate format like “[ $x_1, y_1, z_1$ ], [ $x_2, y_2, z_2$ ]”. Models are then asked to apply geometric operations directly on these points and return the transformed coordinates. This setting removes the complexities of CIF files and serves as a controlled test of whether the LLM can handle spatial transformations at all.

## 2. CIF literacy tests:

- (a) **CIF-Repair:** Evaluates whether the model can recognize and correct corrupted or incomplete CIF files, ensuring basic robustness to noisy inputs. The CIF-Repair task is designed as the most fundamental test of CIF reading ability. The test involves CIF files with common and misleading syntax errors, such as missing tags and wrong tag names, such as “\_cell\_length\_a” being incorrectly written as “\_cell\_length\_x”. The model is expected to correct these errors and produce a valid CIF file. A full list of corruptions is illustrated in Appendix A.6
  - (b) **CIF-Gen:** Evaluates whether the model can explicitly produce syntactically valid CIFs for simple prototype crystals (e.g., sc, fcc, bcc, perovskite), thereby examining familiarity with CIF conventions and basic materials knowledge (as opposed to the open-ended CIF generation explored by Antunes et al. (2024); Chen et al. (2024); Choudhary (2024)).
  - (c) **Chemical Competence Score (CCS):** This test assesses a model’s latent chemical knowledge by evaluating its precision in distinguishing chemically accurate from inaccurate descriptions of crystal structures. While this test is a “perceptual skills” test, we use this to measure the effect that chemistry pretraining has on LLM performance in “motor skills” tasks. Following the methodology of Bran et al. (2025), the dataset was constructed by sampling 600 unique crystal structures from the Materials Project, with corresponding descriptions generated using Robocrystallographer (Ganose & Jain, 2019). An inaccurate dataset was then created by replacing one sentence in each original description with a sentence describing a different crystal. Because the CCS is computed from the token log-likelihoods at the model’s final layer, access to these probabilities is required; this score can be calculated only for locally-run models.
3. **StructProp:** Highlights the deeper challenge of connecting crystal structures with their associated properties. Since properties are determined by structure. This task is not pursued here as a systematic benchmark. Instead, we include StructProp to **underscore the importance of structural understanding as a prerequisite for materials design**, pointing toward the longer-term goal of enabling LLMs to reason about structure-property relationships. For the Struct-Prop task, a model is required to perform actions on a given structure to achieve a desired change direction in a specific property.

## 4 EXPERIMENTAL SETUP

### 4.1 MODELS AND PARAMETER RANGES

**LLMs evaluated:** Gemini 2.5 Pro, GPT-o3, GPT-o4-mini, Deepseek Chat, Llama-3 70B, and Qwen-3 (4B, 8B, 14B, 32B).

Our selection of LLMs covers frontier closed models and strong open-source baselines. We chose the Qwen-3 series to test for parameter scaling effects. We also considered science-specialised LLMs; e.g. NatureLM (Xia et al., 2025), and MatterChat (Tang et al., 2025). However, these were excluded due to either unable to produce outputs in the required CIF format, or not currently accessible via public APIs or code implementations.

For tool-augmented LLMs, we designed a preliminary framework that enables interaction with tools such as Pymatgen. Although this workflow still requires refinement and future iterations may yield stronger results, the current findings already illustrate meaningful trends.

### 4.2 EVALUATION PROTOCOL

Our evaluation is focused on reasoning LLMs. No additional fine-tuning or reinforcement learning was performed. Inference was run with default API parameters. The prompt templates used for all tests can be found in Appendix A.4.

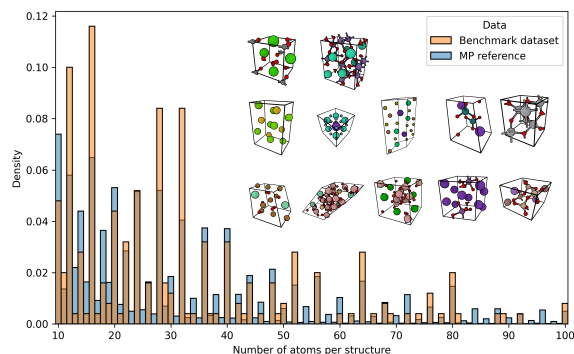


Figure 2: Distribution of the “before” material structures used in AtomMotor-1K (total of 250 structures) by their number of atoms. Also depicted for reference is MP’s distribution and visualisations of some structures used in AtomMotor-1K.

### 4.3 DATASETS

1. **AtomWorld: AtomMotor-1K.** The AtomWorld data generator can in principle produce an unbounded number of test cases. **AtomMotor-1K** is a representative set of 1500 questions. It contains  $5 \times 250$  questions for actions `add`, `move`, `move_towards`, `insert_between`, and `rotate_around`; and  $5 \times 50$  questions for actions `remove`, `change`, `swap`, `delete_below`, and `super_cell`. The CIFs used for “before” states are consistent across action classes as a control. A distribution of these structures by their size is depicted in Figure 2. For the `super_cell` action, the output structure was specified to range from 2 to  $8 \times$  the original cell size. An example of an `insert_between` test is illustrated in Appendix A.5.
2. **PointWorld.** Implemented four AtomWorld-analygous action types - `move`, `move_towards`, `insert_between`, `rotate_around`. Only two points are implemented in one sample, to make the task more fundamental. For each action, 250 samples were tested on Deepseek V3, and 50 samples on Gemini 2.5 Pro. This relatively limited test sample was enough to indicate the pattern of task difficulty in AtomWorld.
3. **CIF-Repair and CIF-Gen.** 22 generated samples for CIF-Repair and 20 manually-labelled samples for CIF-Gen across all LLMs used in AtomWorld. We used only a small scale of tests to isolate the LLM’s understanding of CIF syntax and material structure representation from the demands of AtomWorld tasks.
4. **CCS.** 600 crystal structure descriptions and their corresponding corrupted versions were generated using Robocrystallographer. As only open-source models (Llama-3 70B and Qwen3 series) were tested, the full dataset could be evaluated without the cost constraints of closed-source APIs. This dataset serves to isolate a picture of each model’s latent understanding of crystal structures in natural language.
5. **StructProp.** 209 manually-labelled structures are collected according to Strukturbericht type (Mehl et al., 2017). Due to the testing cost of DFT calculation pipelines, we choose 10 samples to test - for each LLM used in AtomWorld, for each property (band gap and bulk modulus). This was enough to give an indication of how effective LLMs could be for hypothesis-driven CIF modification.

### 4.4 METRICS

1. **Success rate.** Used for all datasets except CCS. Defined as the number of test cases successfully pass all of the following errors divided by the total number of test cases. These errors are categorized into three hierarchical levels:
  - (a) **Wrong output format.** The LLM’s response must enclose the generated structure within a predefined tag so that it can be correctly extracted from the textual output. Failure to do so constitutes an output format error.

- 
- (b) **Wrong structure format.** Even if the structure is successfully extracted, its file format may still be invalid or incompatible with downstream processing tools. Such cases are counted as structure format errors.
  - (c) **Mismatch of structures.** For structurally valid outputs, we compare them with the target structures using `StructureMatcher` with a site tolerance of 0.5. Any generated structure whose site matching exceeds this tolerance is considered a mismatch.
2. **Success rate (StructProp).** The success metric for StructProp includes two additional criterion: whether the generated structure can be used in first principle calculations, and whether the modified structure fulfills the correct property change. A success rate of over 50% for a model indicates the model does better than random guessing.
  3. **Mean maximum distance (`max_dist`).** Used for AtomWorld, PointWorld, CIF-Gen datasets. Computed only for structurally valid outputs that pass the tolerance check. For each matched pair of structures, we calculate the maximum pairwise atomic displacement after optimal alignment, and then average this value across all test cases. The `max_dist` metric is used because it is generally more significant than the RMSD value in our cases. This is because only a few or even a single atom is “moved” while others remain unchanged, making the maximum displacement a more representative indicator of the structural difference.
  4. **CCS score.** This metric was used to evaluate whether LLMs could discern between correct and incorrect crystal structure descriptions. The underlying assumption is that models with a stronger understanding of crystal structures will assign higher likelihoods in their final layer to correct statements than to incorrect ones. Accordingly, the metric measures the separation between the distributions of mean ranks for correct and incorrect descriptions. We report this separation using Cohen’s  $d$  effect size, where larger values indicate a clearer distinction between the two distributions and, by extension, a stronger ability of the model to recognise correct statements based on the provided structure and its surrounding context.

## 5 RESULTS

### 5.1 ATOMWORLD: ATOMMOTOR-1K

The main results of AtomMotor-1K, alongside complementary tests are presented in Figure 3.a. We see some separation of the AtomWorld actions into easy (`change`, `remove`, `swap`, `add`), moderate (`move`, `move towards`, `insert between`) and hard difficulty (`delete below`, `rotate around`) levels based on their success rates. The moderate and hard difficulty tasks constitute greater requirements of multi-step or spatial reasoning. We also notice the mean `max_dist` metric increase for the more difficult tasks (minus tasks not requiring structural perturbations). The `max_dist` distributions for each task are shown in Appendix B.3. One interesting finding is that, the `super_cell` task cannot be well categorised into these difficulty tiers as the success rates range from Llama3-70B’s 4% to 98% from GPT-o3 - it’s both easy (just large-scale repetition) and difficult (requires long-context output) at the same time. The parameter scaling results in Figure 3.c and d illustrate that larger models generally achieve higher success rates and smaller displacements. However, with improvements with scale being marginal with more difficult tasks, and noting that Qwen3-32B outperforms Llama3-70B across most tasks, it suggests that architectural design and training strategies play an equally important role as parameter size. We note that the failure cases appear largely random, with outputs ranging from unmodified input structures to partially modified or slightly perturbed atom positions. A detailed mechanistic analysis would require extensive human inspection and is left for future work.

Our evaluation of our tool-augmented LLM framework on AtomWorld tasks found noticeable gains in model performance. However, the gains are somewhat limited, particularly for more complex actions. Detailed results and comprehensive analysis can be found in Appendix C.

### 5.2 POINTWORLD AND CIF LITERACY TESTS

**PointWorld.** These results are listed in Table 2. Both models are able to reliably output a parseable output with near perfect “success rate” (errors in Deepseek V3 model at `insert_between` tasks are due to it sometimes attempting to write Python scripts instead of performing the calculation).

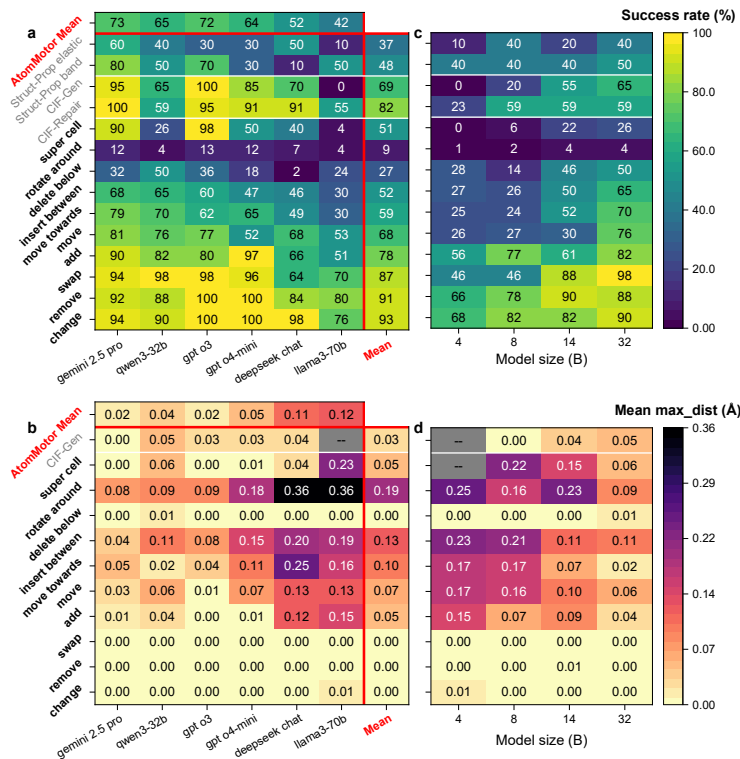


Figure 3: **a.** Success rate metric across AtomMotor-1K, CIF-Repair, CIF-Gen and StructProp datasets. **b.** Mean `max_dist` metric across AtomMotor-1K and CIF-Gen datasets. **c, d.** Parameter scaling results on Qwen3 series. The right side are some randomly sampled structures from the tested data.

The indicator of task difficulty is in the mean `max_dist` scores, where models performed well on `move`, `move_towards`, and `insert_between`, but found `rotate_around` significantly more difficult. The former actions could be solved with straightforward numerical calculations (e.g., addition or weighted averaging), which LLMs can handle reliably. In contrast, models often attempted to compute a rotation matrix for the `rotate_around` action and failed to apply it consistently, leading to high mean `max_dist`.

Table 2: Model performances on simplified point-based tasks. Success rate (Succ. rate) indicates the ratio of unreadable outputs from LLMs. Mean `max_dist` is calculated by the maximum distance between generated and target points after Hungarian sort.

Action	Gemini 2.5 Pro (50 frames)		Deepseek V3-0324 (250 frames)	
	Succ. rate (%)	mean <code>max_dist</code> (Å)	Succ. rate	mean <code>max_dist</code>
<code>move</code>	100.00	0.0000	100.00	0.0000
<code>move_towards</code>	98.00	0.0045	100.00	0.3172
<code>insert_between</code>	100.00	0.0051	78.8	0.0642
<code>rotate_around</code>	98.00	16.168	100.00	14.058

**CIF-Repair.** These evaluations are presented in the main results of Figure 3.a. Most models were able to demonstrate a strong foundational capability in understanding CIF format and errors, with success rates of over 90%. While Llama3 and Qwen3 series have success rates falling below 60%, this does not seem to limit their capability to yield higher success rates even in moderately challenging AtomWorld tasks.

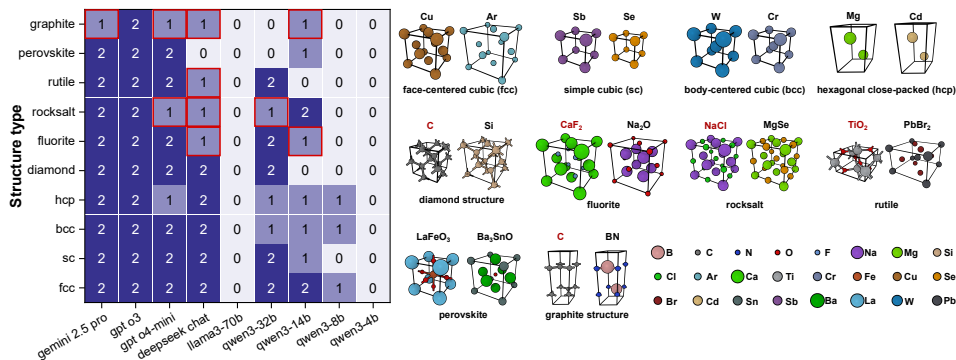


Figure 4: Visualised results of CIF-Gen task. The left side shows the number of correctly generated CIFs for each structure type. The squares marked in red indicate cases where the single correct generation is the standard prototype. The right side shows the specific 3D crystal structures for each type, where the chemical compositions in red represent the standard prototypes.

**CIF-Gen.** These evaluations are presented in the main results of Figure 3.a and show a similar trend to CIF-Repair tasks. A closer look at the error cases in Figure 4 find that chemical compositions that define standard prototypes are generated correctly more often than non-standard compounds that crystallize in the same prototypes (e.g. NaCl vs. MgSe for rocksalt, CaF<sub>2</sub> vs. Na<sub>2</sub>O for fluorite). The fact that asymmetries in training data affect LLMs in this way demonstrates that they rely more on memorization of specific examples rather than understanding the underlying structural principles. Nevertheless, Gemini 2.5 Pro and o3 were able to demonstrate this understanding with success rates of 95% and 100%, respectively.

**CCS.** The resulting scores are reported in Table 3. Similar to AtomWorld, scaling within the Qwen3 series yielded incrementally higher scores, indicating that larger models of the same architectural design acquire a more nuanced grasp of crystal structure properties from their underlying compositions. Notably, while larger Qwen models generally perform better, the Qwen3-32B model surpasses the larger Llama3-70B, mirroring the pattern observed in AtomWorld.

Table 3: CCS score of open-source models

Model	CCS
Qwen3 4B	0.768
Qwen3 8B	0.829
Qwen3 14B	1.061
Qwen3 32B	<b>1.141</b>
Llama3 70b	0.987

### 5.3 STRUCTPROP

These evaluations are presented in the main results of Figure 3.a. Most LLMs were generally unable to get over 50% success rate in these tasks. With the strongest performing model Gemini 2.5 Pro achieving an average success rate of 70%, we list three examples of its reasoning trace in Table 4. These examples highlight LLM knowledge of the definitions of target properties and an ability suggest plausible modification strategies, but also underlines a limited understanding of the underlying electronic structure. In the PtS case, the model correctly identified the key driver of the band gap change as the higher energy of Se 4p compared to S 3p orbitals, but stopped short of a deeper discussion of orbital overlap and covalency - Pt-S bonding is likely to be more covalent than Pt-Se, potentially leading to additional band gap narrowing. In the Ga<sub>2</sub>S<sub>3</sub> case, the model captured the correct trend in terms of electronegativity differences and bond ionicity. The CdAs<sub>2</sub> case highlights an incorrect reasoning flow that still lead to successful completion of the task. The model mischaracterised the relative electronegativities of Cd (1.69) and Zn (1.65), attributing the

Table 4: Excerpts from Gemini 2.5 Pro reasoning trace during successful completions of StructProp tasks. **Correct** and **incorrect** identifications are highlighted.

Structure & Goal	Core thinking process
PtS (mp-288) 	... a potent strategy is to raise the energy of the valence band maximum. This can be achieved by substituting the sulfur atoms with a heavier, less electronegative element from the same group, such as Selenium (Se). <b>The Se 4p orbitals are higher in energy than the S 3p orbitals.</b>
Band gap ↓	
Ga <sub>2</sub> S <sub>3</sub> (mp-539) 	... its band gap is largely determined by the electronegativity difference and bond strength between the Gallium (Ga) cation and the Sulfur (S) anion. <b>To increase the band gap, a modification that strengthens the chemical bonds and increases the material's ionicity is required.</b>
Band gap ↑	
CdAs <sub>2</sub> (mp-471) 	... Cd is a relatively large and electropositive element, leading to bonds with significant ionic character that are less stiff than purely covalent bonds. ... Zn is directly above Cadmium in Group 12 of the periodic table. <b>It has a smaller atomic radius and is more electronegative, which leads to the formation of shorter, stronger, and more covalent bonds with As.</b>
Bulk modulus ↑	

improvement to enhanced ionicity - the true effect is likely linked to stronger covalent bonding due to Zn 3d-As 3p interactions.

---

## 6 DISCUSSION

Isolated tests of PointWorld suggest that LLMs could perform near-perfectly for the simplified `move`, `move_towards`, and `insert_between` tasks - which suggests that the moderate (50-80%) success rate for the AtomWorld analogous tasks is due to difficulty with CIF syntax following as opposed to spatial reasoning. Yet isolated tests for CIF literacy generally found success rates of over 80%, suggesting the opposite - spatial reasoning is more difficult than CIF syntax following. The reality is likely that the task difficulty was compounded when both spatial reasoning and syntax following requirements were combined. Moreover, real-world materials modelling workflows rarely involve single-step actions as in AtomWorld. Instead, they require executing chains of operations. For example, creating supercells is often a prerequisite for other tasks: studying defect properties at a given concentration demands first generating a supercell of appropriate size before atoms can be removed or substituted. A complex instruction such as "generate defect at x% concentration" would thus entail an extended reasoning chain, amplifying the difficulty. Stronger RL specific to AtomWorld tasks could be a solution to helping LLMs understand reasoning chains relevant to CIF modification.

The AtomWorld benchmark is an essential first step: if LLMs cannot reliably perform these basic operations, it will be difficult to envision progress toward more complex materials research workflows. At the same time, solving AtomWorld does not necessarily mean relying on LLMs alone. In practice, difficult actions such as `rotate_around` are better handled by crystallography tools, and future agentic workflows will likely combine LLMs with tool support or multi-modal inputs. Our StructProp results further suggest that current LLMs already show some ability to connect structures with their properties, hinting at the feasibility of gradually scaffolding more complex reasoning within tool-augmented frameworks. From this perspective, AtomWorld can be viewed not as an end in itself but as a foundational stepping stone toward practical, full-cycle agentic materials discovery.

## 7 CONCLUSION

In this paper, we presented AtomWorld as the first benchmark that evaluates LLM motor skills in crystallography. In general, we found that chat models took an algorithmic approach to solving the geometric tasks of our benchmark. With this approach, simpler operations such as `add` could be performed more consistently, whereas more spatially demanding manipulations, particularly rotations, remain highly challenging. These tasks can be solved manually via crystallography software, but for LLMs are an important first stage to enabling higher value tasks such as developing an agentic material discovery workflow. At the same time, preliminary tests suggest that simply equipping LLMs with code tools and RAG is not sufficient to solve problems perfectly. More thoughtful toolflow design and post-training are still necessary for practical application.

LLMs have traditionally struggled with spatial reasoning tasks. However, this may be soon to change with recent developments in tool-augmented design, diffusion, video generation, and language-aligned robotics models (Hu et al., 2025; Song et al., 2025; DeepMind, 2025; Assran et al., 2025). We hope that our AtomWorld playground can play a foundational role in helping researchers of tomorrow test LLMs' understanding of 3D CIF environments.

---

## REFERENCES

- Nawaf Alampara, Santiago Miret, and Kevin Maik Jablonka. Less can be more for predicting properties with large language models, July 2025. URL <http://arxiv.org/abs/2406.17295>. arXiv:2406.17295 [cond-mat].
- Luis M. Antunes, Keith T. Butler, and Ricardo Grau-Crespo. Crystal structure generation with autoregressive large language modeling. *Nature Communications*, 15(1):10570, December 2024. ISSN 2041-1723. doi: 10.1038/s41467-024-54639-7.
- Mido Assran, Adrien Bardes, David Fan, Quentin Garrido, Russell Howes, Mojtaba, Komeili, Matthew Muckley, Ammar Rizvi, Claire Roberts, Koustuv Sinha, Artem Zholus, Sergio Arnaud, Abha Gejji, Ada Martin, Francois Robert Hogan, Daniel Dugas, Piotr Bojanowski, Vasil Khalidov, Patrick Labatut, Francisco Massa, Marc Szafraniec, Kapil Krishnakumar, Yong Li, Xiaodong Ma, Sarath Chandar, Franziska Meier, Yann LeCun, Michael Rabbat, and Nicolas Ballas. V-JEPA 2: Self-Supervised Video Models Enable Understanding, Prediction and Planning, June 2025. URL <http://arxiv.org/abs/2506.09985>. arXiv:2506.09985 [cs].
- Andres M. Bran, Tong Xie, Shai Pranesh, Jeremy Goumaz, Xuan Vu Nguyen, David Ming Segura, Ruizhi Xu, Jeffrey Meng, Dongzhan Zhou, Wenjie Zhang, and Philippe Schwaller. MiST: Understanding the Role of Mid-Stage Scientific Training in Developing Chemical Reasoning Models. In *FM4LS 2025: Workshop on Multi-modal Foundation Models and Large Language Models for Life Sciences at ICML 2025*, July 2025.
- Yan Chen, Xueru Wang, Xiaobin Deng, Yilun Liu, Xi Chen, Yunwei Zhang, Lei Wang, and Hang Xiao. MatterGPT: A Generative Transformer for Multi-Property Inverse Design of Solid-State Materials, August 2024. URL <http://arxiv.org/abs/2408.07608>. arXiv:2408.07608 [cond-mat].
- Kamal Choudhary. AtomGPT: Atomistic Generative Pretrained Transformer for Forward and Inverse Materials Design. *The Journal of Physical Chemistry Letters*, 15(27):6909–6917, July 2024. ISSN 1948-7185, 1948-7185. doi: 10.1021/acs.jpcllett.4c01126. URL <https://pubs.acs.org/doi/10.1021/acs.jpcllett.4c01126>.
- Google DeepMind. Genie 3: A new frontier for world models, May 2025. URL <https://deepmind.google/discover/blog/genie-3-a-new-frontier-for-world-models>.
- Jingru Gan, Peichen Zhong, Yuanqi Du, Yanqiao Zhu, Chenru Duan, Haorui Wang, Carla P. Gomes, Kristin A. Persson, Daniel Schwalbe-Koda, and Wei Wang. Large Language Models Are Innate Crystal Structure Generators, February 2025. URL <http://arxiv.org/abs/2502.20933>. arXiv:2502.20933 [cond-mat].
- Alex M. Ganose and Anubhav Jain. Robocrystallographer: automated crystal structure text descriptions and analysis. *MRS Communications*, 9(3):874–881, September 2019. ISSN 2159-6859, 2159-6867. doi: 10.1557/mrc.2019.94. URL <http://link.springer.com/10.1557/mrc.2019.94>.
- Alex M. Ganose, Hrushikesh Sahasrabudhe, Mark Asta, Kevin Beck, Tathagata Biswas, Alexander Bonkowski, Joana Bustamante, Xin Chen, Yuan Chiang, Daryl C. Chrzan, Jacob Clary, Orion A. Cohen, Christina Ertural, Max C. Gallant, Janine George, Sophie Gerits, Rhys E. A. Goodall, Rishabh D. Guha, Geoffroy Hautier, Matthew Horton, T. J. Inizan, Aaron D. Kaplan, Ryan S. Kingsbury, Matthew C. Kuner, Bryant Li, Xavier Linn, Matthew J. McDermott, Rohith Srinivaas Mohanakrishnan, Aakash N. Naik, Jeffrey B. Neaton, Shehan M. Parmar, Kristin A. Persson, Guido Petretto, Thomas A. R. Purcell, Francesco Ricci, Benjamin Rich, Janosh Riebesell, Gian-Marco Rignanese, Andrew S. Rosen, Matthias Scheffler, Jonathan Schmidt, Jimmy-Xuan Shen, Andrei Sobolev, Ravishankar Sundararaman, Cooper Tezak, Victor Trinquet, Joel B. Varley, Derek Vigil-Fowler, Duo Wang, David Waroquiers, Mingjian Wen, Han Yang, Hui Zheng, Jiongzhi Zheng, Zhuoying Zhu, and Anubhav Jain. Atomate2: modular workflows for materials science. *Digital Discovery*, 4(7):1944–1973, 2025. doi: 10.1039/D5DD00019J. URL <http://dx.doi.org/10.1039/D5DD00019J>.

- 
- S. R. Hall, F. H. Allen, and I. D. Brown. The crystallographic information file (CIF): a new standard archive file for crystallography. *Acta Crystallographica Section A*, 47(6):655–685, 1991. doi: <https://doi.org/10.1107/S010876739101067X>. URL <https://onlinelibrary.wiley.com/doi/abs/10.1107/S010876739101067X>. tex.eprint: <https://onlinelibrary.wiley.com/doi/pdf/10.1107/S010876739101067X>.
- Zhaolin Hu, Yixiao Zhou, Zhongan Wang, Xin Li, Weimin Yang, Hehe Fan, and Yi Yang. OSDA agent: Leveraging large language models for de novo design of organic structure directing agents. In *The thirteenth international conference on learning representations*, 2025. URL <https://openreview.net/forum?id=9YNyiCJE3k>.
- Anubhav Jain, Shyue Ping Ong, Geoffroy Hautier, Wei Chen, William Davidson Richards, Stephen Dacek, Shreyas Cholia, Dan Gunter, David Skinner, Gerbrand Ceder, and Kristin a. Persson. The Materials Project: A materials genome approach to accelerating materials innovation. *APL Materials*, 1(1):011002, 2013. ISSN 2166532X. doi: 10.1063/1.4812323.
- G. Kresse and J. Furthmüller. Efficiency of ab-initio total energy calculations for metals and semiconductors using a plane-wave basis set. *Computational Materials Science*, 6(1):15–50, 1996a. ISSN 0927-0256. doi: [https://doi.org/10.1016/0927-0256\(96\)00008-0](https://doi.org/10.1016/0927-0256(96)00008-0). URL <https://www.sciencedirect.com/science/article/pii/0927025696000080>.
- G. Kresse and J. Furthmüller. Efficient iterative schemes for ab initio total-energy calculations using a plane-wave basis set. *Phys. Rev. B*, 54(16):11169–11186, October 1996b. doi: 10.1103/PhysRevB.54.11169. URL <https://link.aps.org/doi/10.1103/PhysRevB.54.11169>.
- G. Kresse and J. Hafner. Ab initio molecular dynamics for liquid metals. *Phys. Rev. B*, 47(1):558–561, January 1993. doi: 10.1103/PhysRevB.47.558. URL <https://link.aps.org/doi/10.1103/PhysRevB.47.558>.
- G. Kresse and D. Joubert. From ultrasoft pseudopotentials to the projector augmented-wave method. *Phys. Rev. B*, 59(3):1758–1775, January 1999. doi: 10.1103/PhysRevB.59.1758. URL <https://link.aps.org/doi/10.1103/PhysRevB.59.1758>.
- Xiangyan Liu, Bo Lan, Zhiyuan Hu, Yang Liu, Zhicheng Zhang, Fei Wang, Michael Shieh, and Wenmeng Zhou. CodexGraph: Bridging Large Language Models and Code Repositories via Code Graph Databases, 2024. URL <https://arxiv.org/abs/2408.03910>.
- Xiaotong Liu, Yuhang Wang, Tao Yang, Xingchen Liu, and Xiaodong Wen. AlchemBERT: Exploring Lightweight Language Models for Materials Informatics, February 2025. URL <https://chemrxiv.org/engage/chemrxiv/article-details/6781a6b481d2151a02a3212e>.
- Michael J. Mehl, David Hicks, Cormac Toher, Ohad Levy, Robert M. Hanson, Gus Hart, and Stefano Curtarolo. The AFLOW Library of Crystallographic Prototypes: Part 1. *Computational Materials Science*, 136:S1–S828, 2017. ISSN 0927-0256. doi: <https://doi.org/10.1016/j.commat.2017.01.017>. URL <https://www.sciencedirect.com/science/article/pii/S0927025617300241>.
- Andrea Madotto Nate Gruver, Anuroop Sriram and Zachary Ward Ulissi. Fine-tuned language models generate stable inorganic materials as text. In *International conference on learning representations 2024*, 2024.
- Shen Nie, Fengqi Zhu, Zebin You, Xiaolu Zhang, Jingyang Ou, Jun Hu, Jun Zhou, Yankai Lin, Ji-Rong Wen, and Chongxuan Li. Large Language Diffusion Models, February 2025. URL <http://arxiv.org/abs/2502.09992>. arXiv:2502.09992 [cs].
- Andre Niyongabo Rubungo, Kangming Li, Jason Hattrick-Simpers, and Adji Bousso Dieng. LLM4Mat-bench: Benchmarking large language models for materials property prediction. *Machine Learning: Science and Technology*, 6(2):020501, May 2025. ISSN 2632-2153. doi: 10.1088/2632-2153/add3bb. Publisher: IOP Publishing.

- 
- Shyue Ping Ong, William Davidson Richards, Anubhav Jain, Geoffroy Hautier, Michael Kocher, Shreyas Cholia, Dan Gunter, Vincent L. Chevrier, Kristin A. Persson, and Gerbrand Ceder. Python Materials Genomics (pymatgen): A robust, open-source python library for materials analysis. *Computational Materials Science*, 68:314–319, February 2013. ISSN 0927-0256. doi: 10.1016/j.commatsci.2012.10.028.
- John P. Perdew, Adrienn Ruzsinszky, Gábor I. Csonka, Oleg A. Vydrov, Gustavo E. Scuseria, Lucian A. Constantin, Xiaolan Zhou, and Kieron Burke. Restoring the Density-Gradient Expansion for Exchange in Solids and Surfaces. *Phys. Rev. Lett.*, 100(13):136406, April 2008. doi: 10.1103/PhysRevLett.100.136406. URL <https://link.aps.org/doi/10.1103/PhysRevLett.100.136406>.
- Can Polat, Hasan Kurban, Erchin Serpedin, and Mustafa Kurban. Stress-Testing Multimodal Foundation Models for Crystallographic Reasoning. In *Proceedings of the 3rd Workshop on Towards Knowledgeable Foundation Models (KnowFM)*, pp. 49–58, Vienna, Austria, 2025. Association for Computational Linguistics. doi: 10.18653/v1/2025.knowllm-1.5. URL <https://aclanthology.org/2025.knowllm-1.5>.
- Yuxuan Song, Zheng Zhang, Cheng Luo, Pengyang Gao, Fan Xia, Hao Luo, Zheng Li, Yuehang Yang, Hongli Yu, Xingwei Qu, Yuwei Fu, Jing Su, Ge Zhang, Wenhao Huang, Mingxuan Wang, Lin Yan, Xiaoying Jia, Jingjing Liu, Wei-Ying Ma, Ya-Qin Zhang, Yonghui Wu, and Hao Zhou. Seed Diffusion: A Large-Scale Diffusion Language Model with High-Speed Inference, August 2025. URL <http://arxiv.org/abs/2508.02193>. arXiv:2508.02193 [cs].
- Yingheng Tang, Wenbin Xu, Jie Cao, Weilu Gao, Steve Farrell, Benjamin Erichson, Michael W. Mahoney, Andy Nonaka, and Zhi Yao. MatterChat: a multi-modal LLM for material science, 2025. URL <https://arxiv.org/abs/2502.13107>. arXiv: 2502.13107 [cs.AI].
- Joren Van Herck, María Victoria Gil, Kevin Maik Jablonka, Alex Abrudan, Andy S. Anker, Mehrdad Asgari, Ben Blaiszik, Antonio Buffo, Leander Choudhury, Clemence Corminboeuf, Hilal Daglar, Amir Mohammad Elahi, Ian T. Foster, Susana Garcia, Matthew Garvin, Guillaume Godin, Lydia L. Good, Jianan Gu, Noémie Xiao Hu, Xin Jin, Tanja Junkers, Seda Keskin, Tuomas P. J. Knowles, Ruben Laplaza, Michele Lessona, Sauradeep Majumdar, Hossein Mashhadimoslem, Ruaraidh D. McIntosh, Seyed Mohamad Moosavi, Beatriz Mouriño, Francesca Nerli, Covadonga Pevida, Neda Poudineh, Mahyar Rajabi-Kochi, Kadi L. Saar, Fahimeh Hooriabad Saboor, Morteza Sagarichiha, K. J. Schmidt, Jiale Shi, Elena Simone, Dennis Svatunek, Marco Taddei, Igor Tetko, Domonkos Tolnai, Sahar Vahdatifar, Jonathan Whitmer, D. C. Florian Wieland, Regine Willumeit-Römer, Andreas Züttel, and Berend Smit. Assessment of fine-tuned large language models for real-world chemistry and material science applications. *Chemical Science*, 16(2):670–684, 2025. doi: 10.1039/D4SC04401K. Publisher: The Royal Society of Chemistry.
- Wenshan Wu, Shaoguang Mao, Yadong Zhang, Yan Xia, Li Dong, Lei Cui, and Furu Wei. Mind’s Eye of LLMs: Visualization-of-Thought Elicits Spatial Reasoning in Large Language Models, October 2024. URL <http://arxiv.org/abs/2404.03622>. arXiv:2404.03622 [cs].
- Yingce Xia, Peiran Jin, Shufang Xie, Liang He, Chuan Cao, Renqian Luo, Guoqing Liu, Yue Wang, Zequn Liu, Yuan-Jyue Chen, Zekun Guo, Yeqi Bai, Pan Deng, Yaosen Min, Ziheng Lu, Hongxia Hao, Han Yang, Jielan Li, Chang Liu, Jia Zhang, Jianwei Zhu, Ran Bi, Kehan Wu, Wei Zhang, Kaiyuan Gao, Qizhi Pei, Qian Wang, Xixian Liu, Yanting Li, Houtian Zhu, Yeqing Lu, Mingqian Ma, Zun Wang, Tian Xie, Krzysztof Maziarz, Marwin Segler, Zhao Yang, Zilong Chen, Yu Shi, Shuxin Zheng, Lijun Wu, Chen Hu, Peggy Dai, Tie-Yan Liu, Haiguang Liu, and Tao Qin. Nature language model: Deciphering the language of nature for scientific discovery, 2025. URL <https://arxiv.org/abs/2502.07527>. arXiv: 2502.07527 [cs.AI].
- Tong Xie, Yuwei Wan, Yixuan Liu, Yuchen Zeng, Shaozhou Wang, Wenjie Zhang, Clara Grazian, Chunyu Kit, Wanli Ouyang, Dongzhan Zhou, and Bram Hoex. DARWIN 1.5: Large language models as materials science adapted learners, 2025. URL <https://arxiv.org/abs/2412.11970>. arXiv: 2412.11970 [cs.CL].
- Zhuosheng Zhang, Aston Zhang, Mu Li, Hai Zhao, George Karypis, and Alex Smola. Multimodal Chain-of-Thought Reasoning in Language Models, May 2024. URL <http://arxiv.org/abs/2302.00923>. arXiv:2302.00923 [cs].

---

Zangwei Zheng, Xiangyu Peng, Tianji Yang, Chenhui Shen, Shenggui Li, Hongxin Liu, Yukun Zhou, Tianyi Li, and Yang You. Open-Sora: Democratizing Efficient Video Production for All, December 2024. URL <http://arxiv.org/abs/2412.20404>. arXiv:2412.20404 [cs].

## A ATOMWORLD SETUP DETAILS

### A.1 DATASET DISTRIBUTION

Herein, we analyze the distributions of structures collected in our benchmark in terms of elemental composition, number of atoms, number of elements, and space groups, and compare them with those from the Materials Project. The data are shown in Figure 5, Figure 6, Figure 7, and 8, respectively. The structures in our dataset are randomly sampled from the Materials Project, with the number of atoms ranging from 10 to 100. Note that our data generator is not limited to the sampled subset; in principle, any structure file can be used for data generation, and it is capable of automatically generating an unlimited amount of benchmarking data.

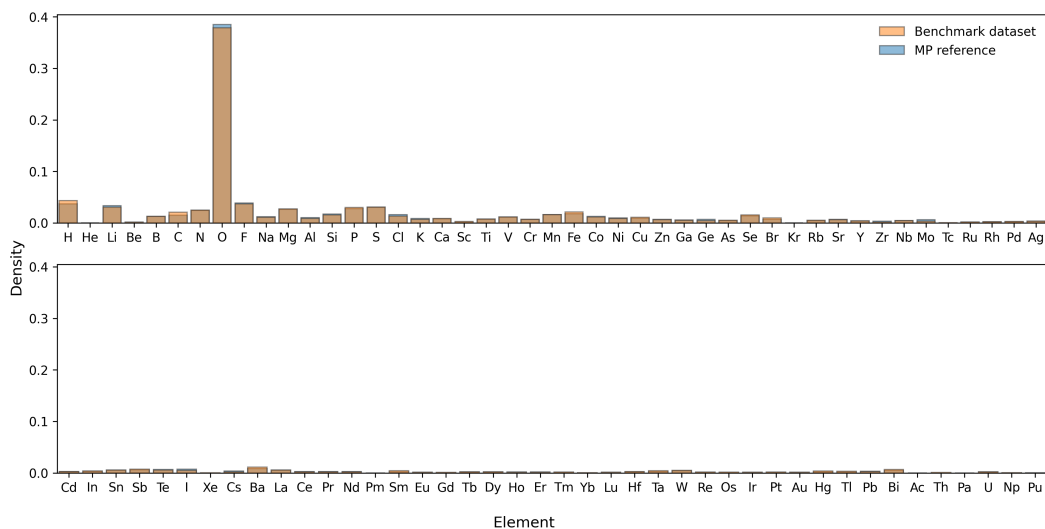


Figure 5: Distribution of structures by elemental composition, compared with the Materials Project. The orange bars represent the data used in the AtomWorld Bench, while the blue bars represent those of the Materials Project.

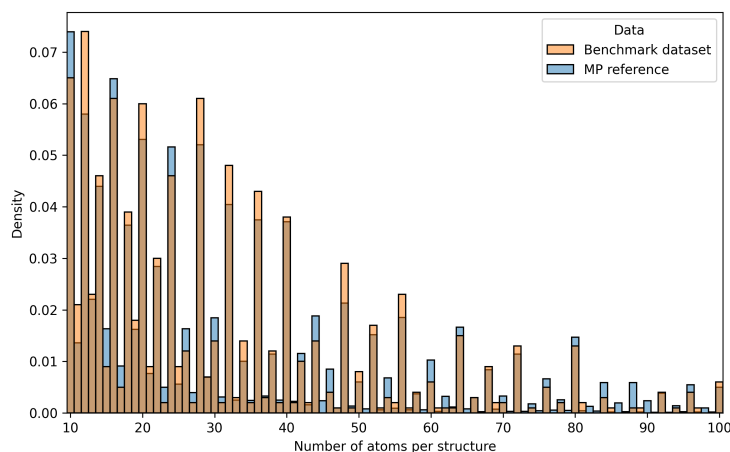


Figure 6: Distribution of structures by the number of atoms, ranging from 10 to 100, compared with the Materials Project.

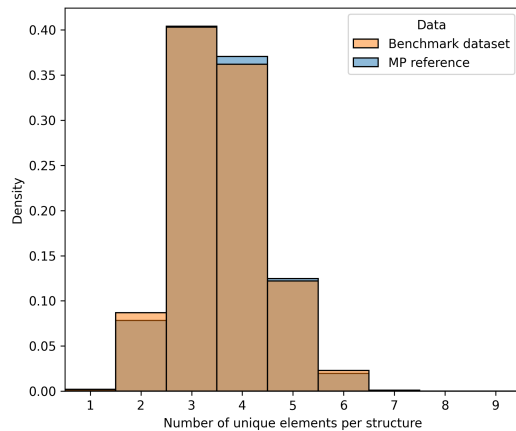


Figure 7: Distribution of the number of elements per structure compared with the Materials Project.

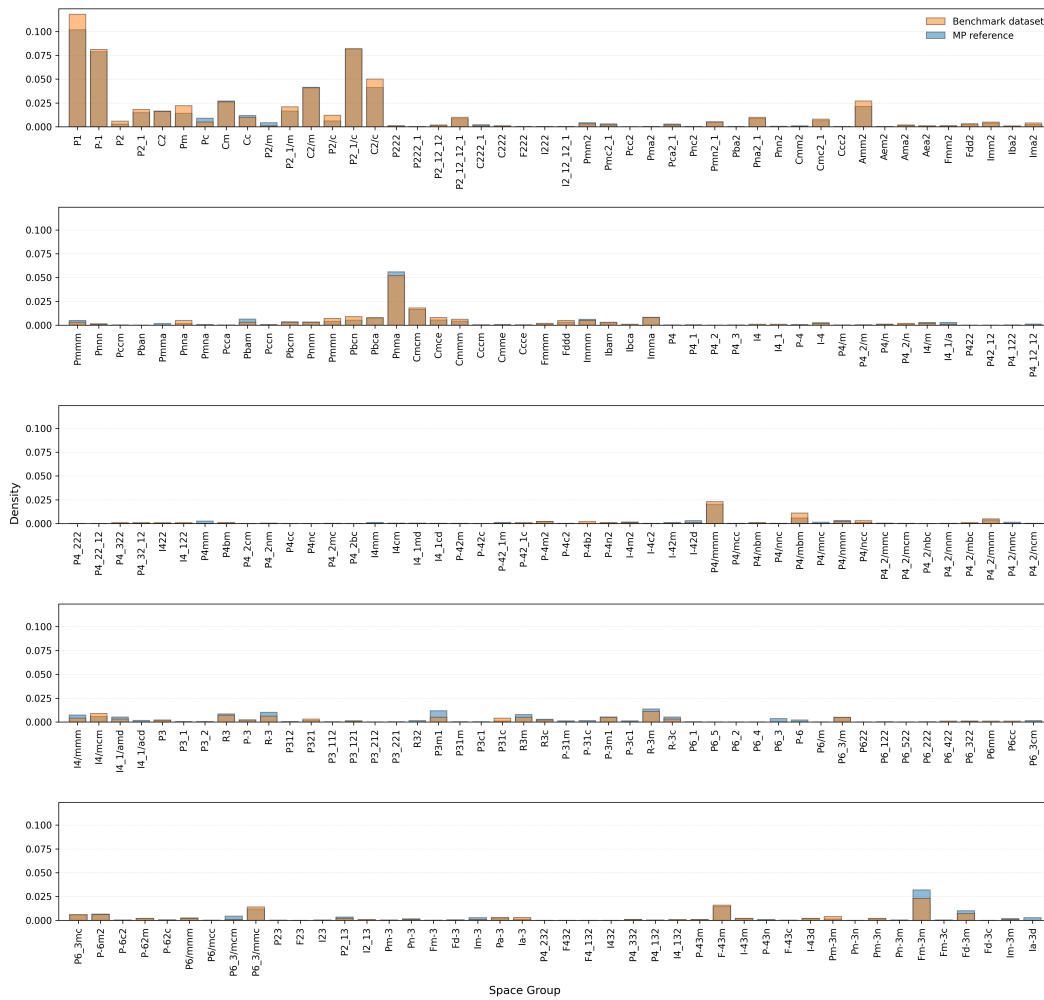


Figure 8: Distribution of structures by space group, compared with the Materials Project.

## A.2 DATA GENERATOR PARAMETERS FOR EACH ACTION

Each action is associated with a set of parameters that specify which atoms the action targets, as well as the magnitude and manner in which the action is applied. Our data generator takes a given structure and a specified action type as input, and produces a set of randomly initialized parameters that define the action. The generator then applies the action to the structure, producing the resulting data. Table 5 lists the parameters required for each action used in this work, along with the ranges from which the data generator randomly samples their initial values.

Table 5: Parameter ranges for random actions in the data generator. The input structure contains  $N$  atoms, and the lattice matrix is  $A = (\mathbf{a}_1, \mathbf{a}_2, \mathbf{a}_3)$ .

Action	Sampling ranges of parameters
change	index: $[0, N)$ symbol: {H, He, ..., Os}
remove	index: $[0, N)$
add	position: $A\mathbf{u}$ , $\mathbf{u} \in [0, 1)^3$ symbol: {H, He, ..., Os}
move	index: $[0, N)$ displacement: $\mathcal{N}(0, \sigma^2 I_3)$ , $\sigma = 2$
move_towards	index1, index2: $[0, N)$ , $\text{index1} \neq \text{index2}$ distance: $[0.1, 3) \text{ \AA}$
insert_between	index1, index2: $[0, N)$ , $\text{index1} \neq \text{index2}$ symbol: {H, He, ..., Os} distance_ratio: $[0.1, 0.9)$
swap	index1, index2: $[0, N)$ , $\text{index1} \neq \text{index2}$ Only between atoms with different symbols.
delete_below	index: $[0, N)$ include_self: {True, False}
rotate_around	index: $[0, N)$ radius: $[1.0, 4.0) \text{ \AA}$ , capped by the structure size. angle: $[45^\circ, 315^\circ)$ axis: $\{\pm\hat{x}, \pm\hat{y}, \pm\hat{z}\}$
super_cell	size: $(a, b, c) \in \{1, 2, 3, 4\}^3$ , $a \times b \times c \leq 8$ , $(a, b, c) \neq (1, 1, 1)$

### A.3 SUPPORTED ACTION PROMPTS FOR POINTWORLD.

Table 6: Examples of actions and the corresponding action prompts for point-based tasks.

Action name	Action prompt
move	Move the point at index {index} by displacement {displacement}.
move_towards	Move the point at index {from_index} towards the point at index {to_index} by {distance}.
insert_between	Insert a new point between points at indices {index1} and {index2}, {distance} units away from point {index1}.
rotate_around	Rotate all points by {angle_deg} degrees around the axis {axis}, with the point at index {center_index} as the center of rotation. The rotation follows the right-hand rule.

### A.4 FULL PROMPT TEMPLATES

Listing 1: A prompt example for a specific task of AtomWorld

```
You are a CIF operation assistant. You will be given an input CIF content
and an action prompt. Your task is to apply the action described in the
action prompt to the initial CIF content. The coordinates in the action
are in Cartesian format. Return the modified CIF content in cif format
within <cif> and </cif> tags.
```

```
Please ensure the output is a valid CIF file, with correct formula, and
atom positions.
```

```
Input CIF content:
{The specific CIF file is inserted here}
```

```
Action prompt: Insert Lu between atoms at indices 6 and 5 that is 4.03
angstrom from atom 6.
```

Listing 2: A prompt example for the PointWorld task

```
You are a spatial reasoning expert. You will be given an initial set of
points and an action prompt describing an operation on these points. The
final modified points after applying the action must be returned inside <
answer> and </answer> tags. The format inside the tags must exactly match
the input points format. All indices are zero-based. Please ensure the
answer inside <answer> and </answer> tags is parseable and strictly
formatted.
```

```
Initial points data:
{coordinate_array},
```

```
Action prompt:
{action_prompt},
```

Listing 3: A prompt example for CIF-repair tasks

```
You are a CIF operation assistant. You will be given a CIF content that
may be corrupted or incomplete. Your task is to examine the CIF content
and fix any issues to ensure it is a valid CIF file. If there are missing
values that cannot be repaired directly, you can use the [
VALUE_TO_BE_INSERTED] as hints to fill in the missing values. Please
ensure the output is a correct CIF file. Return the fixed CIF content
within <cif> and </cif> tags. Input CIF content:
```

```
{broken_cif}
```

#### Listing 4: A prompt example for a CIF-gen task about perovskite structure

You are a materials science expert. Please generate some simple and standard structures in the CIF format according to the requirements. You must strictly follow the CIF format specifications. Since the symmetry-related information can be complex, please write the CIF file with P1 symmetry. Please ensure the output is a correct CIF file. Return the fixed CIF content within `<cif>` and `</cif>` tags.

Requirements:

Please generate a CIF file for {formula} with a {structure\_type} structure, according to the following information about the conventional cell:

- Lattice constant a: {lattice\_constant\_a}
- The {center\_atom} atom is at the center of the octahedron formed by surrounding atoms.

#### Listing 5: A prompt example for StructProp tasks

You are a material design expert. Your task is to modify a given CIF file to achieve a desired change in a specific material property. Please analyze the given CIF file and the target property. Identify the key structural features and elemental composition that influence the specified property. Propose a specific modification to the structure. This modification must be one or a combination of the following:

1. Element Substitution;
2. Lattice Parameter Adjustment;
3. Atomic Coordinate Adjustment.

Please ensure the output is a correct CIF file. Return the modified CIF content within `<cif>` and `</cif>` tags.

Input CIF content:

{The specific CIF file is inserted here}

Your goal: modify the CIF file accordingly to {target\_trend} the {target\_property}.

#### A.5 ILLUSTRATIVE EXAMPLE OF THE FRAMEWORK

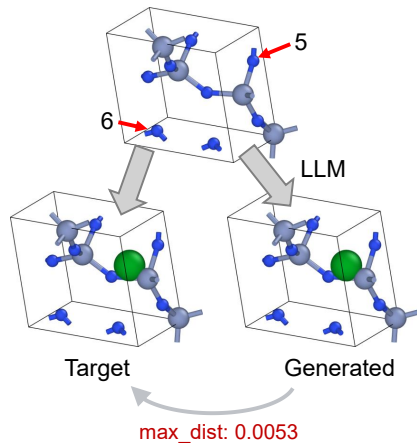


Figure 9: The workflow of a specific insert\_between task.

To provide a concrete understanding of our proposed AtomWorld Bench, we present an illustrative example of its workflow. This case study focuses on a specific task: inserting a Lu atom between the fifth and the sixth atoms in the specific CIF structure. The prompt used here is listed in Appendix A.4.

---

The workflow randomly selects the atom indices and determines the position of the atom to be inserted based on the selected atoms. Based on the initialized action, the framework gives out a target structure. The LLM will also generate a structure after processing the prompt, as shown in Figure 9. In this example, the two structures are nearly identical, with a `max_dist` of 0.0053 Å, indicating high accuracy.

#### A.6 LOGIC ON GENERATING CIF-REPAIR TASK

To systematically evaluate LLM performance on CIF repair, we constructed a set of partially corrupted CIFs via two types of operations:

1. **Removal of essential lines:** Certain CIF fields are critical for correct structure parsing. The essential tags include:
  - `_cell_length_a`, `_cell_length_b`, `_cell_length_c`
  - `_cell_angle_alpha`, `_cell_angle_beta`, `_cell_angle_gamma`
  - `_atom_site_type_symbol`, `_atom_site_label`,  
`_atom_site_symmetry_multiplicity`
  - `_atom_site_fract_x`, `_atom_site_fract_y`, `_atom_site_fract_z`
  - `_atom_site_occupancy`
2. **Replacement of essential tags with misleading variants:** Instead of random typos, tags are systematically replaced with misleading but syntactically valid alternatives. Examples of mappings include:
  - Change the `a`, `b`, `c` into `x`, `y`, `z`; `u`, `v`, `w` or `i`, `j`, `k`.
  - Change the `x`, `y`, `z` into `a`, `b`, `c`; `u`, `v`, `w` or `i`, `j`, `k`.
  - Change `_atom_site` string into `_atom`.
  - Change `_cell` string into `_lattice`.
  - Change `_cell_length` and `_cell_angle` strings into `_cell`.

#### A.7 DFT COMPUTATION DETAILS

All density functional theory (DFT) calculations, including band gap and bulk modulus evaluations, were performed using the Vienna Ab initio Simulation Package (VASP) with the projector-augmented wave (PAW) method (Kresse & Hafner, 1993; Kresse & Furthmüller, 1996a;b; Kresse & Joubert, 1999) and the PBEsol exchange–correlation functional (Perdew et al., 2008). High-throughput workflows for both properties were automated using the `atomate2` package (Ganose et al., 2025). Unless otherwise specified, calculation parameters followed the default settings in `atomate2`. Example calculation scripts are provided in the github repository.

For the band gap calculations, a k-point mesh with a grid density of  $100 \text{ \AA}^{-3}$  was employed, and electronic self-consistency was converged to  $10^{-5}$  eV. The band gap was extracted from the uniform k-point calculation stage. For the bulk modulus calculations, a plane-wave energy cutoff of 600 eV and a k-point grid density of  $400 \text{ \AA}^{-3}$  were used. Total energy and ionic relaxations were converged to  $10^{-6}$  eV and 0.01 eV/Å, respectively, to balance computational cost and accuracy. In the initial relaxation stage, Gaussian smearing with  $\sigma = 0.05$  eV was applied, while in the deformation stage the tetrahedron method was adopted for Brillouin zone integration.

---

## B SUPPLEMENTARY EXPERIMENTAL DATA

### B.1 PROMPT CHOICE AND MISINTERPRETATION

During tests, we found that certain prompt formulations could cause LLMs to misinterpret spatial actions as text-level editing, specifically for the `swap` action (Listing 6). Prompts that focused on textual “indices” without explicitly framing the task as a spatial transformation caused some models to attempt CIF-text rewriting instead of manipulating atomic coordinates. To verify whether this was an intrinsic ambiguity in the wording, we asked three domain experts in materials modelling to perform the same tasks using only the less explicit prompt. Both interpreted the action correctly and did not exhibit the LLM-style misinterpretation. As domain experts with long-term experience in atomic modelling, their prior exposure to structure manipulation likely provides an additional intuition for identifying the spatially intended reading, rather than a purely textual one. In contrast, LLMs appear to exhibit a default “interpretive bias” toward textual position unless the spatial nature of the task is made explicit.

Our goal, however, was not to optimize prompts, but to ensure consistent and unambiguous task interpretation. All experiments therefore use a single unified prompt set, chosen simply to remove obvious sources of misunderstanding while maintaining comparability across tasks. These prompts are likely not globally optimal but effectively prevent semantic confusion without engaging in extensive prompt tuning.

Listing 6: Less explicit and explicit spatial prompts for `swap` action

<p><b>Less explicit prompt:</b> "Swap atoms at indices {self.index1} and {self.index2} in the cif file. The indices of atoms are started from 0."  Success rate (Deepseek-chat): <b>22%</b> Success rate (Qwen3 32B): <b>50%</b></p> <p><b>Explicit spatial prompt:</b> "Swap <b>the spatial positions</b> of atoms at indices {self.index1} and {self.index2} in the cif file. The indices of atoms are started from 0."  Success rate (Deepseek-chat): <b>64%</b> Success rate (Qwen3 32B): <b>98%</b></p>
--

### B.2 PERFORMANCE SENSITIVITY ANALYSIS

#### B.2.1 SENSITIVITY ON THE NUMBER OF ATOMS

To quantitatively investigate the influence of the number of atoms on the action success rate, we prepared test data that is as clean as possible, using a single action with consistent and simple action parameters. For the structures, we employed different supercell sizes of the same base structure. For each structure, we have tested 10 times. In this case, we chose the `insert_between` action to insert a Hydrogen atom in the middle between atoms at indices 3 and 5. We chose BiOF (mp-762304,  $P2_1/c$ , 12 atoms per unit cell) as the test system, and generated supercells with 12, 24, 48, 96, 144, and 216 atoms. This system was selected to provide moderate structural complexity while being representative of a three-element compound with ample data in the Materials Project.

As shown in Figure 10, the success rates of all tested models decrease as the number of atoms in the CIF increases. The larger model (Qwen3 32B) shows a slower decline compared to the smaller ones (Qwen3 4B). Beyond 200 atoms, all three models failed in every test case. This trend suggests that while larger models are more robust to increasing input size, extremely large structures still exceed the models’ effective reasoning capacity.

#### B.2.2 SENSITIVITY ON BRAVAIS LATTICE TYPES

We also investigated the effect of structural symmetry on the action success rate. Given that there are 230 space groups in total, analyzing all of them would be impractical. Therefore, we focused on the

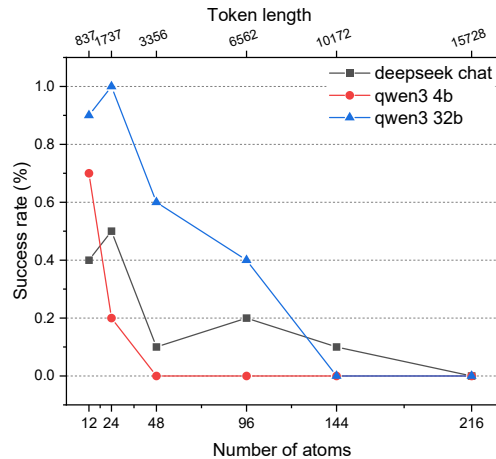


Figure 10: The relation between success rate and the number of atoms (directly related to token lengths).

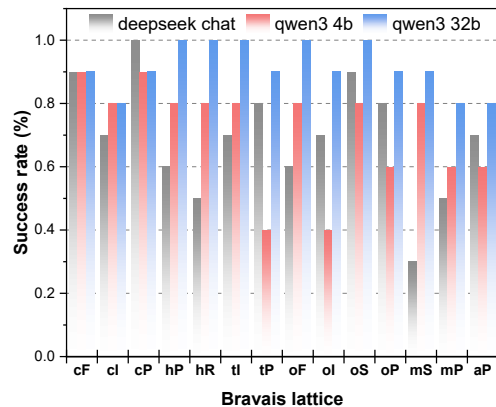


Figure 11: The success rate under the 14 Bravais lattice types.

14 Bravais lattices for statistical analysis. To minimize the influence of other factors, we performed random sampling from the Materials Project, selecting conventional cells containing 12 to 28 atoms, and collected 10 structures for each lattice type. As shown in Figure 11, the Bravais lattices are arranged roughly in decreasing order of symmetry, from face-centered cubic (cF) to simple primitive (aP). The success rates of the three tested models show no clear correlation with the lattice symmetry. However, the models tend to achieve slightly lower accuracy on low-symmetry systems, although a definitive conclusion would require more detailed investigation.

### B.2.3 SENSITIVITY ON THE ACTION POSITIONS

We further evaluated whether the position of the target atom in the CIF sequence affects the action success rate. To this end, we prepared paired test cases using the same structure, where the target atoms appeared either early or late in the CIF atom list. All other factors were kept fixed. Specifically, we used the `insert_between` action with a `distance_ratio` of 0.45 and fixed the inserted atom type as Hydrogen. For the “early” setting, the selected atom indices were 0 and 1, whereas for the “late” setting, the last two indices in the CIF were used. The underlying structures are identical to those used in the standard `insert_between` tasks.

As shown in Table 7, the tested models consistently achieve higher success rates when the target atoms appear earlier in the CIF sequence. Although the difference is not large, the trend is observed across the two evaluated models. Overall, the results indicate that atom ordering has some impact on performance, but the effect remains limited under our testing conditions. To overcome this issue, we believe that the future agentic systems should use specific tools or modalities to understand the structures, then perform the actions.

Table 7: The success rate for different action positions.

Action position	Deepseek-chat (%)	Qwen3 32B (%)
Index 0, 1	90	96
Index -2, -1	82	80

#### B.2.4 PERFORMANCE ON MOVING ALL ATOMS

We further evaluated the `move_all` action, which requires the model to translate the entire structure by a specified displacement vector. As summarized in Table 8, the success rates of all tested models drop substantially compared to the single-atom `move` tasks. In many failed cases, the generated structures show noticeable randomness in the atomic positions, indicating that the models have difficulty performing consistent global translations.

Unlike the other main metrics in AtomWorld, evaluating `move_all` poses an additional challenge: a rigid translation preserves the structure up to translational symmetry. As a result, the standard `StructureMatcher` cannot be directly applied because it intentionally factors out translational degrees of freedom. To quantify deviations, we implemented a custom metric similar to `StructureMatcher` but without enforcing translational invariance, comparing atoms by their index correspondence and computing the resulting coordinate deviations.

Table 8: The metrics for the `move_all` action.

Models	Success rate (%)	mean <code>max_dist</code> (Å)
Deepseek-chat	54	0.1111
Qwen3 4B	12	0.1118
Qwen3 8B	24	0.0252
Qwen3 14B	40	0.0467
Qwen3 32B	46	0.0487

#### B.3 THE `MAX_DIST` VIOLIN PLOTS

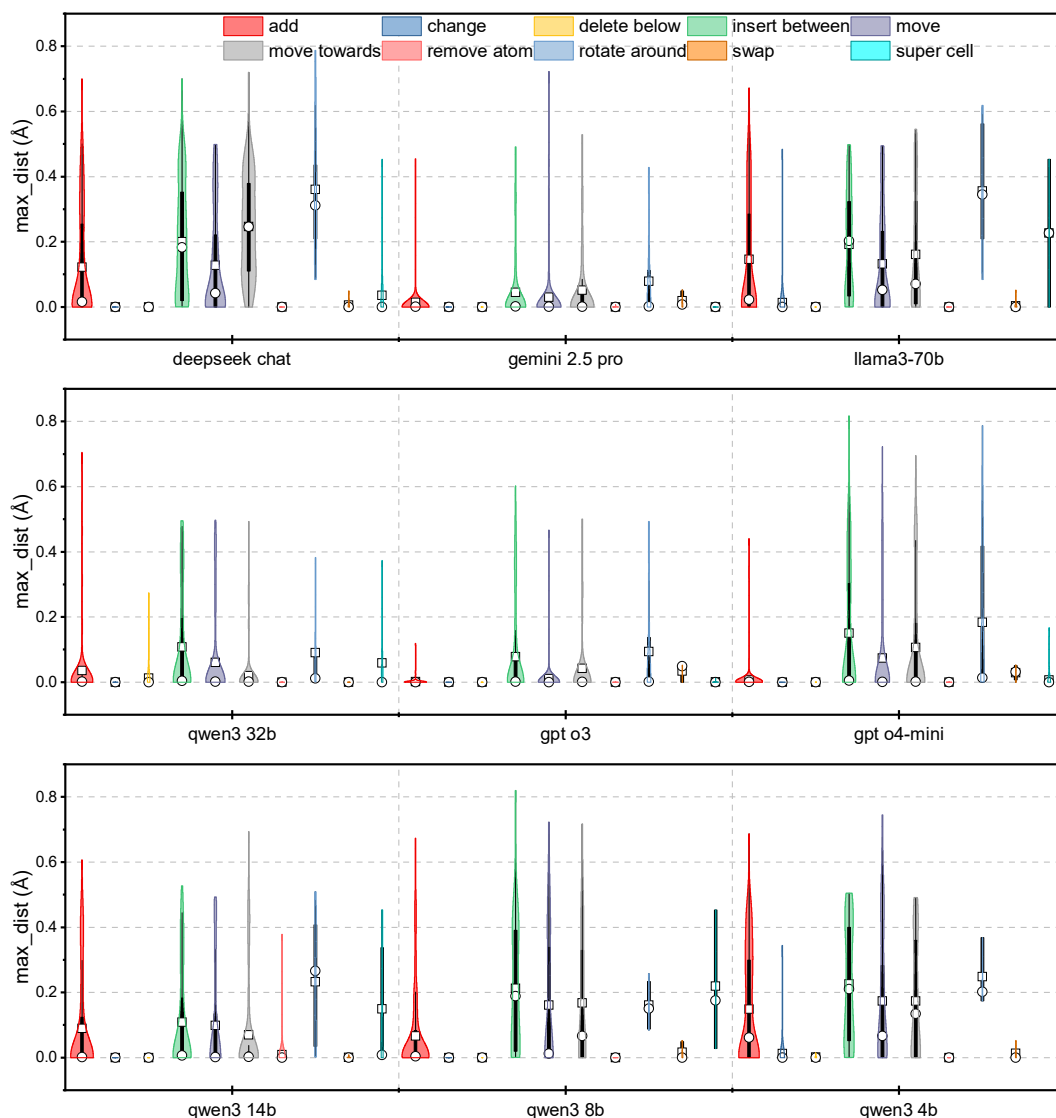


Figure 12: The violin plots of `max_dist` of evaluation results. The hollow squares indicate the mean values, and the hollow circles indicate the medians.

## C EVALUATIONS OF TOOL AUGMENTED LLM FOR ATOMWORLD

**System Design** As shown in Figure 13, we adopt a code generation-based approach to accomplish structural operations. This process is divided into two steps: first, we perform RAG-based retrieval over the `pymatgen` library to obtain relevant APIs; second, we conduct code generation to complete the user-specified action.

**Knowledge Graph Retrieval (RAG)** The first step of our pipeline is to retrieve relevant `pymatgen` APIs using RAG. We leverage the `code-graph-rag` project (Liu et al., 2024) to extract structured information from the codebase and build a knowledge graph in Memgraph, where nodes represent code entities such as modules, classes, methods, and fields, and edges capture relationships like inheritance and usage. The retrieval process is orchestrated by a primary LLM, implemented using Deepseek-chat, which performs task decomposition, reasoning, and tool invocation. Specifically, the translator LLM, also implemented with Deepseek-chat, is used as a tool by the primary LLM

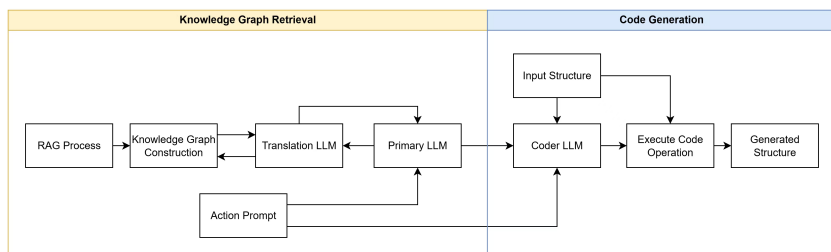


Figure 13: The flowchart for the code generation-based approach for the AtomWorld benchmark tests.

to convert natural language queries into graph queries. The output of this process is a JSON file containing relevant pymatgen APIs, which is later used to guide code generation.

**Code Generation** Code generation is performed using Deepseek-chat, conditioned on the input CIF file, the user action prompt, and the APIs retrieved from the RAG stage. The system strictly follows the retrieved API signatures to ensure correctness and prevent hallucination. The generated Python code is then executed together with the input CIF file to produce the modified crystal structure.

Table 9: Comparison of model performances between Deepseek-chat with and without tools.

Action	With tools		Without tools	
	Succ. rate (%)	mean max_dist (Å)	Succ. rate	mean max_dist
remove	<b>100.0</b>	0.0000	84.0	0.0000
insert_between	<b>83.0</b>	0.0076	45.6	0.2004
rotate_around	<b>18.0</b>	0.1648	6.8	0.2561

As evident from Table 9, incorporating retrieval-augmented generation (RAG) and structure manipulation tools significantly improves the model’s performance across the tested actions. The `remove` action, which is relatively straightforward, achieves a perfect success rate of 100%. However, more complex actions, such as `insert_between` and `rotate_around`, still present challenges. The success rate for `insert_between` is 83%, with some errors remaining, while `rotate_around` demonstrates a relatively low success rate of 18%.

These findings highlight a key insight: while the integration of RAG tools and coding ability facilitates substantial improvements in model performance, further refinements are crucial to fully address the real-world requirements of structural modification tasks. Specifically, additional task-specific fine-tuning or reinforcement learning is necessary to enhance the model’s robustness, particularly for more complex structural operations. Future work will focus on these aspects to ensure more reliable and scalable applications.